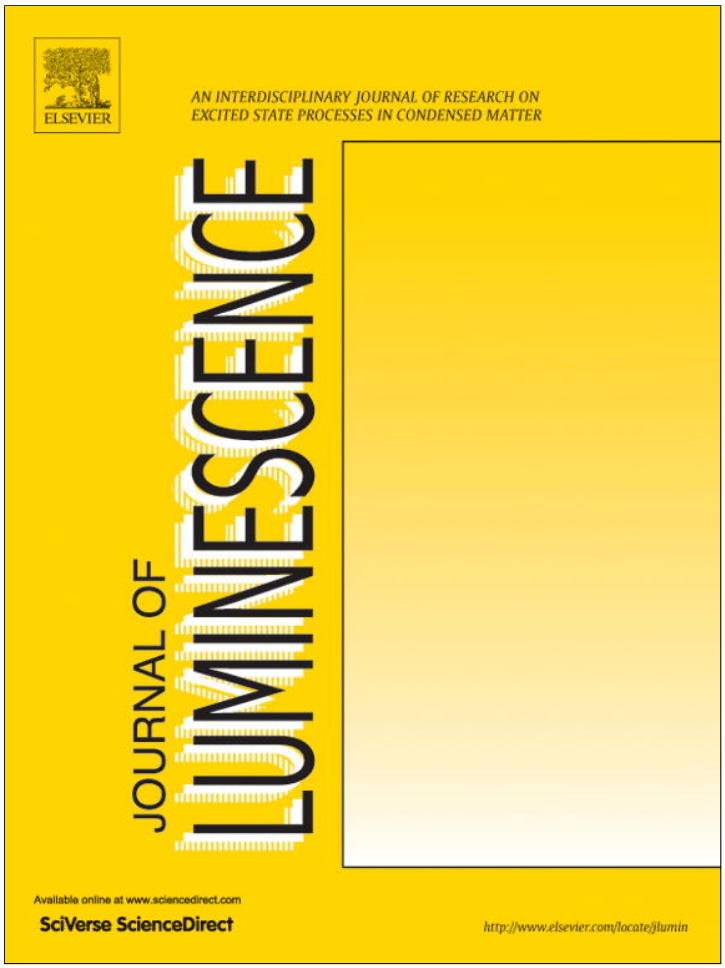

Journal of Luminescence 143 (2013) 43–49

Contents lists available at SciVerse ScienceDirect

Journal of Luminescence

journal homepage: www.elsevier.com/locate/jlumin

Metal-enhanced fluorescence of mixed coumarin dyes by silver and gold nanoparticles: Towards plasmonic thin-film luminescent solar concentrator

S.M. El-Bashir [a,b,*], F.M. Barakat [a], M.S. AlSalhi [a]

[a] Department of Physics & Astronomy, Science College, King Saud University, Riyadh, KSA, Saudi Arabia
[b] Department of Physics Faculty of Science, Benha University, Egypt

ARTICLE INFO

Article history:
Received 5 December 2012
Received in revised form
1 April 2013
Accepted 18 April 2013
Available online 27 April 2013

Keywords:
Plasmonic luminscent solar concentrator
PMMA thin films
Metal enhanced fluorescence
Silver and gold nanoparticles

ABSTRACT

Poly(methyl methacrylate) (PMMA) nanocomposite films doped with mixed coumarin dyestuffs and noble metal nanoparticles (60 nm silver and 100 nm gold) were prepared by spin coating technique. The effect of silver and gold nanoparticles on the film properties was studied by Fourier transform infrared spectroscopy (FT-IR), differential scanning calorimetry (DSC), transmission electron microscopy (TEM), scanning electron microscopy (SEM), UV–vis absorption and fluorescence spectroscopy measurements. DSC measurements indicated the increase of the glass transition temperature of the films by increasing nanogold concentration, recommending their promising thermal stability towards hot climates. It was found that the fluorescence signals of the mixed coumarin dyes were amplified by 5.4 and 7.15 folds as a result of metal enhanced fluorescence (MEF). The research outcomes offered a potential application of these films in solar energy conversion by plasmonic thin film luminescent solar concentrator (PTLSC).

1. Introduction

1.1. Luminescent solar concentrators (LSCs)

Solar power is considered as a prime candidate for alternative energy sources since the annual average solar radiation in the world has its maximum value of about 7 kW h/m^2.day; in view of that the potential for solar photovoltaics is enormous [1]. Despite the fact that the photovoltaic (PV) technology is improving rapidly and the methods of manufacturing more efficient PV cells are being developed, but the industry is still being hampered by the cost [2]. The best approach to reduce the cost of PV power is basically to reduce the number of PV cells by concentrating sunlight; therefore, the price of a photovoltaic system can be considerably less important [3]. Common ways of concentrating photovoltaic (CPV) systems involve using lenses and mirrors which have a considerable heating effect on PV cells and consequently cooling systems are needed to avoid the decrease in the conversion efficiency as the temperature is increased [4]. Another disadvantage for traditional concentrators is the tracking system which add a significant cost to PV system [5]. An alternative method of concentrating light is the use of luminescent solar concentrators (LSCs) which made up of luminescent species doped in a transparent substrate, usually glass or plastic, with photovoltaic cells placed around the edges [6–9]. Light photons enters the face of the substrate where it is absorbed by the luminescent molecule then fluoresces photon at a longer wavelength, which is waveguided via total internal reflection to the edge of the substrate where it can be absorbed by the photovoltaic cell [10–12]. The main advantage of LSC is the idea of covering the area with a luminescent transparent plate is far cheaper than the coverage with solar panels specially in building integrated PV systems [13]. Additionally, LSCs do not require sun tracking because they collect efficiently diffused light as well as the direct light [14]. A more aesthetically beneficial aspect of LSCs is that they can be easily incorporated into windows, thus using the light that is not absorbed by the dye to illuminate rooms indoors [15].

1.2. Thin film LSCs

Fig. 1 shows the construction and the operation principle of Thin film LSCs have several other advantages that they allow the absorption of the full solar spectrum by the stacking several luminescent layers which are containing different types of luminescent species [16]. In addition flexible employments of thin-film LSCs can be made on any commercial host substrate; making them of a great economic value [17]. The main drawback of thin film LSCs is the decrease of the absorption of solar radiation by small film thickness This problem could be solved using the plasmonic properties of noble (Au, Ag) metal nanoparticles (MNPs). MNPs are known to possess interesting properties called surface plasmon

* Corresponding author at: Department of Physics & Astronomy, Science College, King Saud University, Riyadh, KSA, Saudi Arabia. Tel.: +966 565850487; fax: +966 14673656.
E-mail address: elbashireg@yahoo.com (S.M. El-Bashir).

0022-2313/$ - see front matter © 2013 Elsevier B.V. All rights reserved.
http://dx.doi.org/10.1016/j.jlumin.2013.04.029

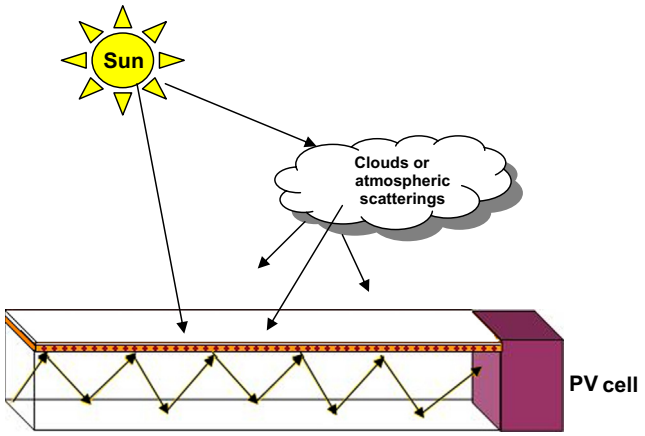

Fig. 1. Thin-film luminescent solar concentrator: Top layer antireflection coating, mid layer fluorescent film and bottom layer transparent plate.

resonance (SPR) bands in the visible region of the electromagnetic spectrum. This property arises due to the collective oscillations of the conduction band electrons induced by incident electromagnetic radiation. The frequency and shape of SPR bands are strongly dependent on the size and shape of metal nanoparticles (MNPs) as well as on the dielectric constant of the surrounding media [18]. The ability of MNPs to amplify fluorescence signals and increase a fluorophore's quantum yield has brought about important changes to fluorescence spectroscopy as well as to its applications [19]. It was found that the maximum amplification occurred when the wavelength of SPR of metal nanoparticle coincides with that of the fluorescence band of the dye molecule. The metal–fluorophore interactions has flourished as it was found that the optical properties of these fluorophores could be modulated by plasmonic interactions [20].

This paper aims to develop metal-enhanced fluorescence (MEF) by SPR between stabilized Ag-NPs, Au-NPs and mixed coumarin dye molecules doped in PMMA films. There are many potential advantages of using Ag-NPs and Au-NPs for MEF because of their chemical and thermal stability. All these information will finally be used to discuss and demonstrate the aspects of a promising implication, regarding the application of the prepared films in the manufacturing of PTLSCs.

2. Experimental techniques

2.1. Materials

PMMA was obtained from (Aldrich, USA). Coumarin dyestuffs MACROLEX Fluorescent Red G and MACROLEX Fluorescent Yellow 10GN were obtained from (Bayer, Germany). Spherical gold and silver nanoparticles Ag-NPs and Au-NPs with average particle diameters 60 nm and 100 nm were obtained from Aldrich (USA). HPLC grade Dichloromethane (CH_2Cl_2) was obtained from Aldrich (USA) and used as high purity solvent for PMMA grains.

2.2. Fluorescent PMMA films

PMMA grains and coumarin dyestuffs were dissolved in dichloromethane (CH_2Cl_2) and mixed by a magnetic stirrer at 40 °C for 6 h. The polymer solution was doped by different concentrations (ppm) of Coumarin dyestuffs MACROLEX Fluorescent Red G and MACROLEX Fluorescent Yellow 10GN. All the dye doped polymer solutions were sonicated for 6 h before pouring on glass substrates and spin coated in a centrifuge at 2000 rpm for 1 min to obtain uniform film coverage [18], then they are left to dry in an electric oven at 40 °C for 6 h. The film thicknesses were measured using a profilometer (Talystep, Taylor Hobson, UK) on a scratch made immediately after deposition of five independent measurements on each sample, and found to be in the range of 50 ± 10 μm [21].

2.3. Metal enhanced fluorescent PMMA films

The optimized fluorescent PMMA film was determined by fluorescence measurements and found to have dye concentrations of 70 ppm MACROLEX Fluorescent Yellow 10GN and 30 ppm MACROLEX Fluorescent Red G, respectively. The fluorescence spectra of optimized fluorescent PMMA film was enhanced by spherical Ag-NPs and Au-NPs doped as received with different concentrations (ppm) using the same procedure described before.

2.4. Characterization and measurements

FT-IR spectra for all samples were recorded in the wave number range (4000–400 cm^{-1}) with an FT-IR spectrophotometer (Genesis Series, USA). The nanoparticle distribution was examined by the transmission electron microscope (TEM), (JEOL JEM-1400, Japan) and scanning Electron Microscope (SEM) (JEOL, JSM-5400, Japan). The absorption spectra were recorded in the wavelength range (190–900 nm) using a UV–vis spectrophotometer (UNICAM, Helios Co., Germany). The steady-state fluorescence spectra were recorded in the wavelength range (400–800 nm) using a spectrofluorimeter (Perkin Elmer LS 50 B, UK).

3. Results and discussion

3.1. Material characterization

Fourier transform infrared spectroscopy (FT-IR) was used in order to know some information about the interactions between the vibrational energy states of Ag-NPs, Au-NPs, coumarin and PMMA molecules. Fig. 2 shows the FT-IR transmission spectra in the wavenumber range (4000–400 cm^{-1}), before and after doping with 20 ppm Ag-NPs and Au-NPs. It is noted that all the spectra neat and doped PMMA films are almost identical without noticeable shifts in the positions of the vibrational peaks of the characteristic groups [22]. The behavior observed in the spectra can be attributed to the fact that the nanoparticle concentrations are too small to make any observable effects on the chemical bonds of PMMA, reflecting the chemical stability of the PTLSC films since all the physical properties of PMMA films can be retained after doping with noble metal nanoparticles.

Fig. 3 shows TEM images for Ag-NPs and Au-NPs used as received, it is clear that all the nanoparticles are spherical and close to each other with the affinity to form aggregates. Therefore the nanoparticles were sonicated for enough time in the polymer solution in order to obtain a homogeneous coating to prepare PTLSC waveguides. The optimal sonication time for Ag-NPs and Au-NPs suspended in the dye doped PMMA/CH_2Cl_2 solution was found to be 6 h determined by SEM photographs shown in Fig. 4. It is clearly noticed that all Ag-NPs and Au-NPs exhibit regular smooth spherical shape with a slight change in the mean diameter of the nanospheres, this convinced that the sonication process is important to reduce the probability of cluster formation [10].

3.2. Spectroscopic properties of PMMA films doped with mixed coumarin dyestuffs

Fig. 5 shows the absorption spectra of MACROLEX dyes before and after being mixed in PMMA film with concentration 50 ppm of

each dye. Two absorption bands are observed the first observed at 450 nm characterizing (Yellow 10 GN) and second at 520 nm characterizing (Red G). It was suggested that, the position of the absorption band is determined only by the chain length and by the number of π electrons of the dye molecules [23]. It is also observed that the dye mixture absorb broadly over the visible region of solar spectrum, thus a considerable amount of sunlight can be converted. The optimum concentration ratios for the dye mixtures will be determined by the fluorescence spectroscopy measurements in order to detect the optimum mixing concentration ratios which strongly affect the performance PTLSCs.

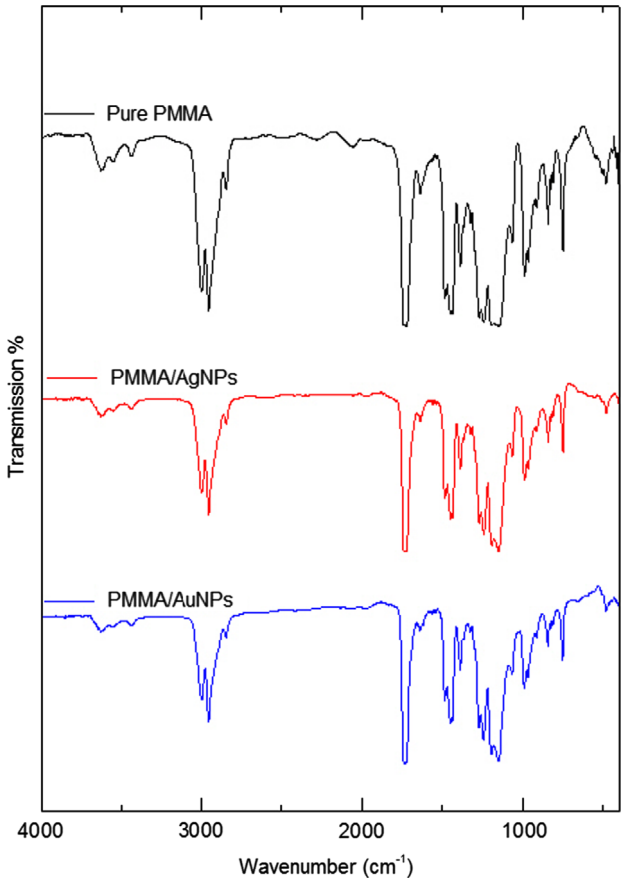

Fig. 2. FT-IR spectra for neat and 20 ppm nanoparticle doped PMMA films.

Fig. 6 illustrates the fluorescence spectra of fluorescent PMMA films doped with different concentrations of MACROLEX fluorescent dyes. The spectra of both dyes show a strong dependence on the concentration, giving the highest fluorescence intensity for 70 ppm (Yellow 10 GN) and 30 ppm (Red G). Above these concentrations, an abrupt reduction in the fluorescence intensity accompanied with a red shift had been occurred. The formation of these new bands may be originated from the existence of other electronic states which are completely different from those of a single dye molecule [24]. The absolute fluorescence quantum yield "ϕ_F" and Stokes shift "$\Delta\lambda_s$" of fluorescent PMMA films were calculated as mentioned in Ref. [25] using equations,

$$\phi_F = \phi_{ref}(a/a_{ref})(n/n_{ref})(S_{ref}/S) \quad (1)$$

$$\Delta\lambda_s = \lambda_{F(max)} - \lambda_{a(max)} \quad (2)$$

where ϕ_{ref} is the fluorescence quantum yield of the standard sample (reference), a is the absorbance, n is the refractive index of the matrix and S is the area under the fluorescence curve, $\lambda_{F(max)}$ and $\lambda_{a(max)}$ are the wavelengths at the fluorescence and absorbance maxima, respectively, the values $\Delta\lambda_s$ and ϕ_F are listed in Tables 1 and 2. The observed decrease in ϕ_F accompanied with rise in $\Delta\lambda_s$ values by increasing dye concentrations can be mainly attributed to the formation of excited state dimers (two bonded dye molecules) and higher aggregates which have small values of ϕ_F [25]. The strength of the aggregation depends mainly on the dye nature, the host media and the factors related to the preparation conditions [26]. In other words, the dimer fluorescence is more predominant than that of the monomer if they are equally present in the polymer matrix [10].

From the previous study, we determined the dye concentrations (70 ppm Yellow 10GN and 30 ppm Red G) for preparing the optimized fluorescent PMMA film in order to increase the absorption of visible solar spectrum. The excitation wavelength of this film was determined by applying a Gaussian least square fitting of the measured absorption spectrum, the fitting showed one absorption maximum of the mixture at 490 nm, as shown in Fig. 7.

3.3. *Enhancing the fluorescence spectra of PMMA films by surface plasmons*

Ag-NPs and Au-NPs of 60 nm and 100 nm diameters were selected for enhancing the fluorescence of coumarin dyes since MNPs have broad absorption spectra overlapped with the fluorescent spectra of MACROLEX fluorescent dyes as illustrated by Fig. 8. This selection was made on the basis of MEF occurrence by

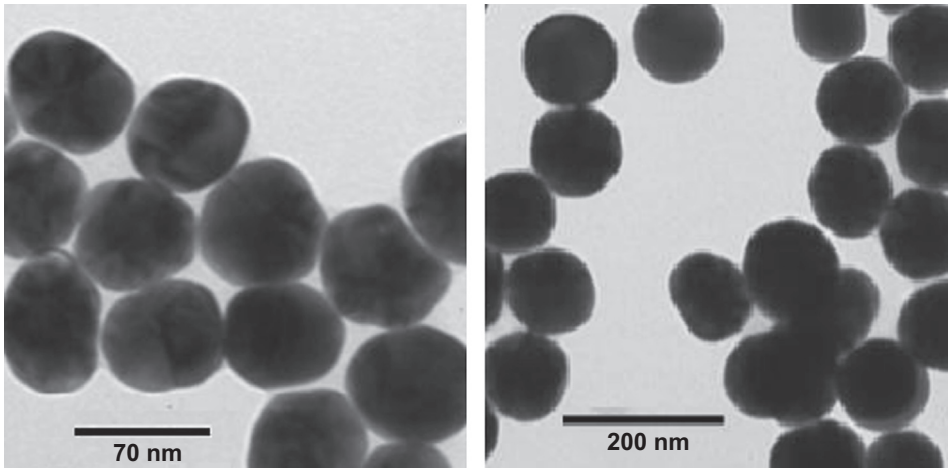

Fig. 3. TEM images for the as received Ag-NPs (left) and AuNPs (right).

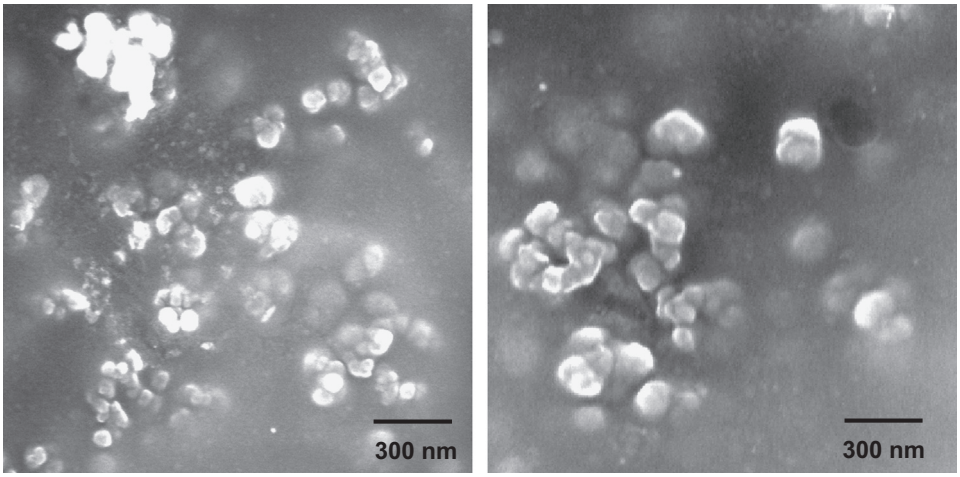

Fig. 4. SEM images for Ag-NPs (left) and Au-NPs (right) dispersed in PMMA/CH_2Cl_2 solution.

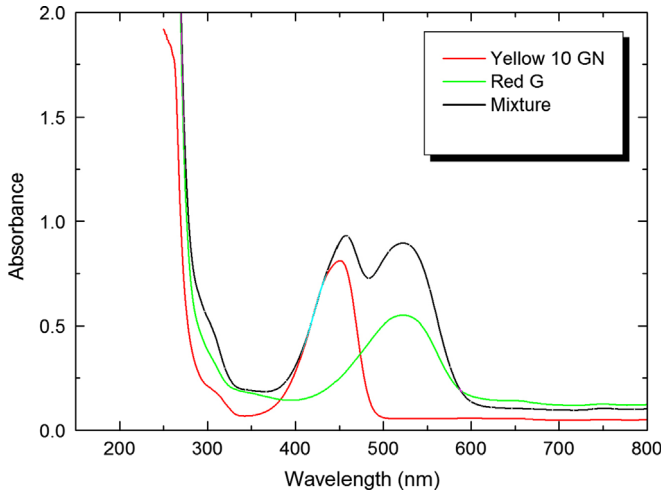

Fig. 5. Absorption spectra of MACROLEX fluorescent dyes before and after mixing in PMMA film with concentration 50 ppm. (For interpretation of the references to color in this figure legend, the reader is referred to the web version of this article.)

the coincidence between the absorption and fluorescence maxima of MNP and the dye molecule, respectively [20,27].

The effect of Ag-NPs concentration on the fluorescence spectra of the optimized fluorescent film (PMMA/70 ppm Yellow 10GN/30 ppm Red G) is illustrated in Fig. 9. It is observed that the fluorescence intensity is increased by adding Ag-NPs without changes in the spectrum shape, this confirms the uniform dispersion of Ag-NPs in the polymer matrix [28]. It can also be noticed that the fluorescence intensity depends sensitively on the nanoparticle concentration, since the fluorescence intensity is enhanced by increasing Ag-NPs concentration up to 20 ppm and then reduced. This can be explained by the fact that the spacing between the optical emitter (dye molecule) and the metal nanoparticle is another important factor that controls the plasmonic interaction and consequently the fluorescence intensity [20]. If the dye molecules are too close to MNP (less than a few nanometers), then the possibility exists that the excited state electrons and holes can tunnel to the Ag-NPs through nonradiative relaxation [28]. Therefore, the optimum spacing should be exist and controlled by MNP concentration, as has been observed in the fluorescence intensity of fluorescent PMMA film doped with 20 ppm Ag-NPs which enhanced by 2.4-folds for the two signals of MACROLEX dyes. More efforts had to be done for further

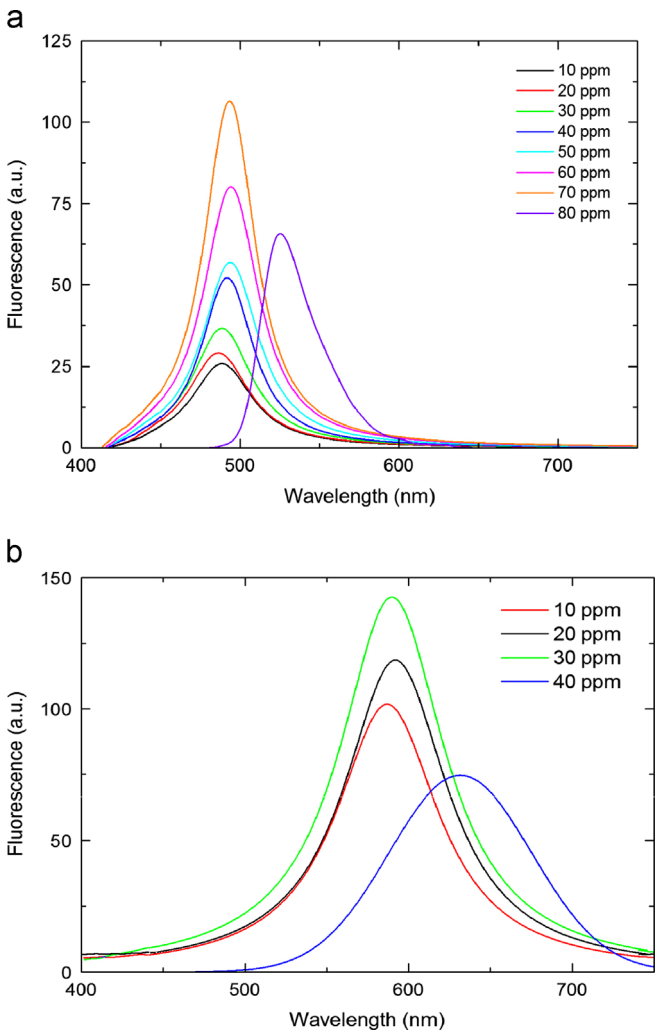

Fig. 6. The fluorescence spectra of PMMA films doped with MACROLEX fluorescent coumarin dyestuffs: (a) MACROLEX Fluorescent Yellow 10GN and (b) MACROLEX Fluorescent Red G. (For interpretation of the references to color in this figure legend, the reader is referred to the web version of this article.)

enhancing of the fluorescence band concerning coumarin (Red G), this will done by using large Au-NPs due to their chemical stability and strong surface plasmon oscillations in the visible range of electromagnetic spectra [29].

Table 1
Fluorescence quantum yield and Stokes shift for PMMA films doped with MACROLEX Fluorescent 10GN.

Concentration (ppm)	ϕ_F	$\Delta\lambda_s$ (nm)
10	0.28	42
20	0.35	44
30	0.44	47
40	0.51	51
50	0.64	54
60	0.71	58
70	0.86	64
80	0.62	75

Table 2
Fluorescence quantum yield and Stokes shift for PMMA films doped with MACROLEX Fluorescent Red G.

Concentration (ppm)	ϕ_F	$\Delta\lambda_s$ (nm)
10	0.58	68
20	0.79	72
30	0.90	79
40	0.61	108

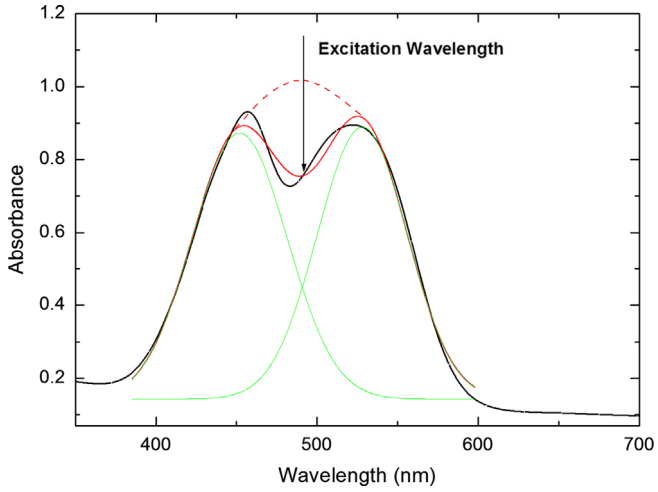

Fig. 7. Gaussian fitting of the absorption spectra of mixed MACROLEX fluorescent dyes in PMMA film.

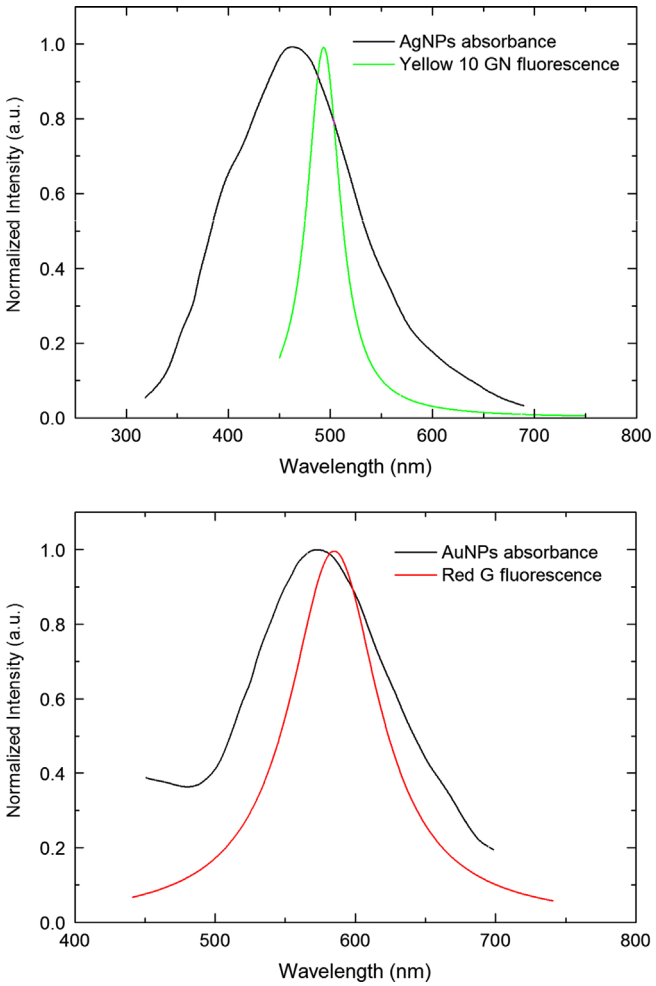

Fig. 8. The absorption spectra of Ag-NPs and Au-NPs compared to the fluorescence spectra of MACROLEX dyes.

Fig. 10 shows the effect of Au-NPs concentration on the fluorescence spectra of (70 ppm Yellow 10GN/30 ppm Red G/20 ppm Ag-NPs) doped PMMA film. Further 3 and 4.75 folds amplification of the fluorescence intensity was attained for the florescent dyes Yellow 10GN and Red G, respectively. Thus, it can be realized that the fluorescence signals were enhanced by 5.4 and 7.15 folds as a consequence of metal enhanced fluorescence which follows the plasmon resonance spectrum of Ag-NPs and Au-NPs. Two mechanisms are considered in the literature responsible for the fluorescence enhancement: (a) the electromagnetic field enhanced near metallic nanoparticles due to the localized surface plasmon resonance (LSPR) at the surface of the MNPs and (b) the coupling between the molecular dipole of the dye molecules and the surface plasmon field of the metal [30]. The LSPR modifies the intensity of the electromagnetic field around the fluorophore and this can lead to an increase in the emitted fluorescence intensity. The latter effect leads to an increase of the radiative decay rate, determining a stronger fluorescence emission, phenomenon known as radiative decay engineering (RDE) [31]. Other important factors which could affect the strength of the fluorescence enhancement via LSPR are the size and shape of the nanoparticles, the degree of overlapping between LSPR and the emission band of the dye as well as the value of the quantum yield (ϕ_F) of the fluorescent molecule [32].

3.4. Indoor thermal stability testing

DSC measurements were performed for PTLSC films (PMMA/70 ppm MACROLEX Fluorescent Yellow 10GN, 30 ppm MACROLEX Fluorescent Red G, 20 ppm Ag-NPs) doped by different concentrations of Au-NPs. The glass transition temperature, T_g, was determined by the endothemic peak depicted on Fig. 11. It is clearly observed that the value of T_g is shifted from 105 °C to 126 °C by increasing the concentration of Au-NPs from 5 ppm to 25 ppm. This can be explained as the incorporation of fillers into the polymeric matrix can make changes in the physical characteristics of the resulting nanocomposite [33]. These changes have been reported for composites containing a wide range of fillers and polymers, but most recently for composites containing nanosized fillers. Some researchers affirmed the increase in the value of T_g of composites upon increasing filler content [34–36], but decreases have also been stated [35,36]. From this study it can be confirmed that the thermal stability of PTLSCs can be improved by increasing

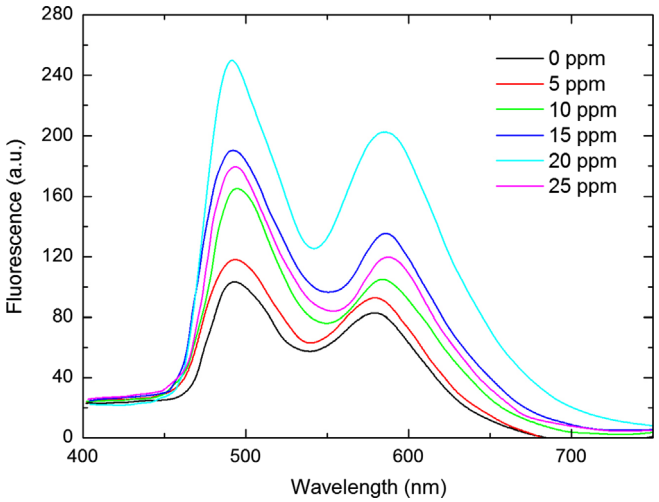

Fig. 9. Effect of Ag-NPs concentration on the fluorescence spectra of PMMA film doped with mixed MACROLEX dyes (70 ppm Yellow 10GN/30 ppm Red G). (For interpretation of the references to color in this figure legend, the reader is referred to the web version of this article.)

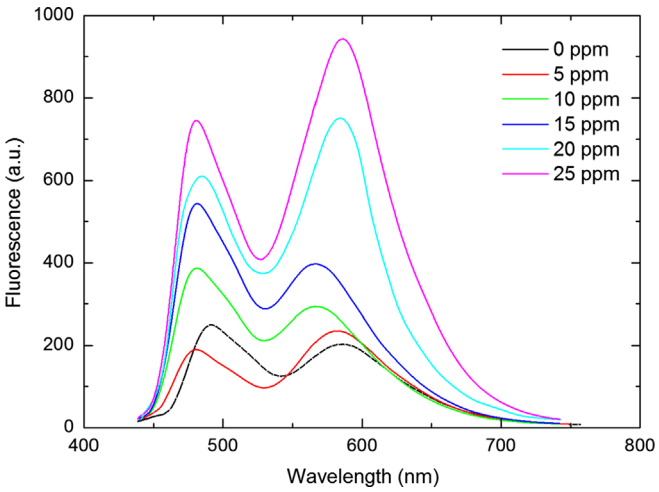

Fig. 10. Effect of Au-NPs concentration on the fluorescence spectra of fluorescent PMMA films doped with (70 ppm Yellow 10GN/ 30 ppm Red G/ 20 ppm Ag-NPs). (For interpretation of the references to color in this figure legend, the reader is referred to the web version of this article.)

nanogold concentration, this behavior recommends the thermal stability of PTLSC films in outdoor applications.

4. Conclusions

This paper reports on the metal enhanced fluorescence of two mixed coumarin dyestuffs (MACROLEX) doped in PMMA films for PTLSC applications. Our results showed a 2.4- folds amplification of the two fluorescence signals by modifying the electromagnetic field around the fluorescing molecules by increasing the concentration of 60 nm Ag-NPs up to 20 ppm and then reduced at higher concentrations. This can be ascribed to the fact that the enhanced field decays exponentially as increasing the spacing between the fluorescing molecules and MNPs, so fluorescing molecules located in the range of the enhanced field experience plasmonic interaction. Additional 3 and 4.75 folds magnification of enhanced fluorescence was achieved by using 100 nm Au-NPs, this can be

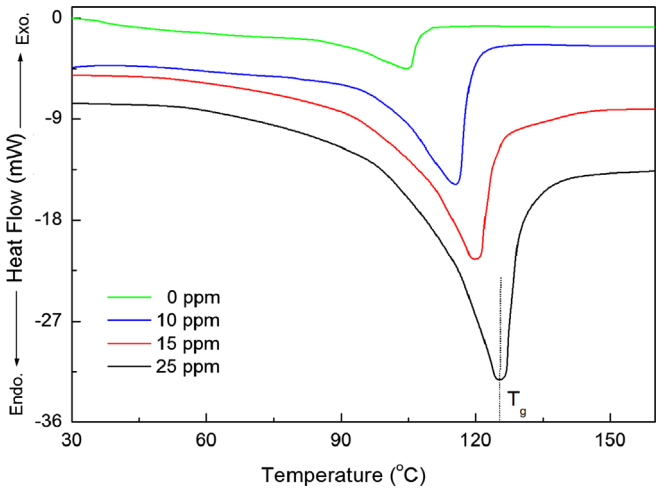

Fig. 11. Effect of DSC AuNPs concentration on the thermograms for PMMA doped with (70 ppm Yellow 10GN, 30 ppm Red G, 20 ppm AgNPs). (For interpretation of the references to color in this figure legend, the reader is referred to the web version of this article.)

due to the linear increase of the mixed plasmon absorption maximum with the Au-NPs concentration, this provides a very convenient way of tuning the optical absorption properties [37]. The photophysical properties of the optimized films suggests them as potential candidates for PTLSC applications.

Acknowledgement

This research project was supported by a grant from the Research Center of the Center for Female Scientific and Medical Colleges in King Saud University.

References

[1] G.B. Smith, C.G. Granqvist, Green Nanotechnology—Solutions for Sustainability and Energy in the Built Environment, Taylor & Francis Inc., 2010.
[2] M.A. Green, Third Generation Photovoltaics: Ultra-High Efficiency at Low Cost, Springer-Verlag, 2003.
[3] G.K. Oberlehner, M. Bardosova, M. Pemble, B.S. Richards, Sol. Energy Mater. Sol. Cells 104 (2012) 53.
[4] P. Würfel, Physics of Solar Cells: From Basic Principles to Advanced Concepts, WILEY-VCH Verlag GmbH & Co., 2009.
[5] M.G. Debije, P.C. Verbunt, B.C. Rowan, B.S. Richards, T.L Hoeks, Appl. Opt. 47 (2008) 6763.
[6] B.C. Rowan, L.R. Wilson, B.S. Richards, IEEE J. Sel. Top. Quantum Electron. 14 (2008) 1312.
[7] J. Bomm, et al., Sol. Energy Mater. Sol. Cells 95 (2011) 2087.
[8] G. Maggioni, A. Campagnaro, S. Carturan, A. Quaranta, Sol. Energy Mater. Sol. Cells 108 (2013) 27.
[9] M.G. Debije, P.P.C. Verbunt, Adv. Energy Mater. 2 (1) (2012) 12.
[10] S.M. El-Bashir, J. Lumin. 132 (2012) 1786.
[11] F.P. Milton, Y.K. Gun'ko, J. Mater. Chem. 22 (2012) 16687.
[12] W.H. Weber, J. Lambe, Appl. Opt. 15 (1976) 2299.
[13] J.W.E. Wiegman, E. van der Kolk, Sol. Energy Mater. Sol. Cells 103 (2012) 41.
[14] A. Goetzberger, W. Greubel, Appl. Phys. A: Mater. Sci. Process. 14 (1977) 123.
[15] G.B. Smith, Sol. Energy Mater. Sol. Cells 84 (2004) 395.
[16] W.G.J.H.M. van Sark, Renewable Energy 49 (2013) 207.
[17] T. Dienel, C. Bauer, I. Dolamic, D. Brühwiler, Sol. Energy 84 (2010) 1366.
[18] N.S. Basheera, B.R. Kumara, A. Kuriana, S.D. George, J. Lumin. 137 (2013) 225.
[19] J.R. Lakowicz, Anal. Biochem. 337 (2005) 171.
[20] S. Chandra, J. Doran, S.J. McCormack, M. Kennedy, A.J. Chatten, Sol. Energy Mater. Sol. Cells 98 (2012) 385.
[21] A. Pepe, P. Galliano, M. Aparicio, A. Duran, S. Cere, Surf. Coat. Technol. 200 (2006) 3486.
[22] S. Srivastava, M. Haridas, J.K. Basu, Bull. Mater. Sci. 31 (2008) 213.
[23] F.P. Shäfer, Dye Lasers, Springer-Verlag, New York, 1990.
[24] J.F. Rabek, Experimental Methods in Polymer Chemistry, JohnWiley &Sons, 1980.

[25] J.R. Lakowicz, Principles of Fluorescence Spectroscopy, second ed., Kluwer Academic, Plenum Press, New York, 1999.
[26] M. Hammam, M.K. El-Mansy, S.M. El-Bashir, M.G. El-Shaarawy, Desalination 209 (2007) 244.
[27] Y. Chen, K. Munechika, D.S. Ginger, Nano Lett. 7 (2007) 690.
[28] O. Kulakovich, et al., Nano Lett. 2 (2002) 1449.
[29] V. Levchenko, M. Grouchko, S. Magdassi, T. Saraidarov, R. Reisfeld, Opt. Mater. 34 (2011) 360.
[30] J.R. Lakowicz, Anal. Biochem. 298 (2001) 1.
[31] J.R. Lakowicz, Anal. Biochem. 324 (2004) 153.
[32] C.D. Geddes, J.R. Lakowicz, J. Fluoresc. 12 (2002) 121.
[33] F.K. Liu, S.Y. Hsieh, F.H. Ko, T.C. Chub, Colloids Surf., A 231 (2003) 31.
[34] C. Becker, H. Krug, H. Schmidt, Mater. Res. Soc. Symp. Proc. 435 (1996) 235.
[35] W. Hergeth, U. Steinau, H. Bittrich, G. Simon, K. Schmutzler, Polymer 30 (1989) 254.
[36] B.J Ash, L.S. Schadler, R.W. Siegel, Mater. Lett. 55 (2002) 83.
[37] S. Link, Z.L. Wang, M.A. El-Sayed, J. Phys. Chem. B 103 (1999) 3529.